

Enrichment of W₂B₅ from WO₃ and B₂O₃ by Double SHS Method

Bora DERIN*, Sertac YAZICI

Metallurgical and Materials Engineering Department, Istanbul Technical University, Maslak, Istanbul, 34469, Turkey

crossref <http://dx.doi.org/10.5755/j01.ms.24.1.17834>

Received 27 March 2017; accepted 01 May 2017

A second self-propagating high-temperature synthesis (SHS) was carried out to enrich the W₂B₅ content in the SHS product containing a mixture of various tungsten boride compounds. In the experiment, the process called Double-SHS (D-SHS) was conducted in two steps. In the first SHS reaction, an initial molar composition ratio of WO₃:B₂O₃:Mg mixture was selected as 1:3:8. The product was then hot-leached with hydrochloric acid to eliminate MgO and Mg₃B₂O₆ phases. The leached product, consisting of 72.6 wt.% W₂B₅, 16.1 wt.% WB, 8.4 wt.% W₂B, and 2.9 wt.% W, was again reacted with the Mg and B₂O₃ mixture by second SHS. After another acid leaching step, W₂B₅ content in the D-SHS product was found to be 98.2 wt.%. The study showed that D-SHS is an effective method for boron enrichment in the tungsten compounds.

Keywords: W₂B₅, WO₃, double SHS, leaching, XRD.

1. INTRODUCTION

Tungsten borides (W₂B, WB, W₂B₅, and W₄B) and their composites are useful refractory compounds on account of their high hardness, chemical inertness, electronic conductivity and resistance to thermal shock [1–6]. In the literature, there are many studies about the coating, cutting, sintering and electronic properties of these compounds [1–12]. Tungsten borides are mostly synthesized by solid state reaction between W and amorphous B powder pressed in compacts at elevated temperatures, e.g. pretreatment at 500 °C in hydrogen for 1 hour followed by 800–1200 °C in argon for 2 hours [12]. A few other production methods that may be feasible are mechanical alloying, molten salt electrolysis, vapor deposition and arc melting [5–13].

Self-propagating high-temperature synthesis (SHS) is an alternative technique that can be used for the productions of many refractory compounds such as carbides, nitrides, silicides, intermetallics, oxides etc. [14]. Sub-micron and nano-sized powders can be also produced by this method [15–17]. A low initiation energy requirement, very fast processing rate, and simple operation enhance the significance of SHS process. In the SHS process, after initiation, the reaction propagates in the reactant mixture and proceeds in the self-propagating mode. Especially for the thermite-type SHS processes, the adiabatic temperature value (T_{ad}) is an important indicator to estimate whether a reaction is self-propagating or not [14]. Depending on the raw materials used for the SHS process, acid leaching may be required to eliminate unwanted compounds in the SHS product [18]. In our previous studies, we produced tungsten boride product as a mixture of W₂B, WB, and W₂B₅ by SHS method and following acid leaching techniques starting from CaWO₃ or WO₃ as cheap sources of tungsten [18, 19]. It was concluded in the studies that, even if the simultaneous

additions of B₂O₃ and Mg to the initial mixture increased the atomic ratio of boron to tungsten in the boride formations, single step SHS was not enough to eliminate all metallic tungsten and sub-borides such as W₂B and WB due to the nature of SHS. Besides, these additions lead to not only an increase in the quantity of Mg₃B₂O₆, which is more difficult to leach than MgO, but also to a slow dissolution rate and high temperature requirement in the leaching step.

The present process, named D-SHS, covers a leaching and second SHS/leaching trials on the previously produced SHS product [19]. The aim is to increase B/W ratio and to obtain a final product with high grade of W₂B₅ which has notable improvements in mechanical properties and wear resistance of some composites [7, 20].

2. EXPERIMENTAL STUDY

The chemical composition of the initial raw materials and the experimental procedure for the first-SHS are also described elsewhere [19]. In the study, WO₃ (Alfa Aesar Co., 99.8 % pure with particle size < 106 µm), B₂O₃ (99 % pure with particle size < 53 µm) and Mg (99.7 % pure with particle size < 150 µm) powders were used. After the drying of the powders at 110 °C for 2 hours, the 50 g of initial mixture was prepared at the molar ratio of WO₃:B₂O₃:Mg as 1:3:8 and charged into the MgO crucible. After compaction, tungsten resistance wire was placed on the mixture surface. The crucible was closed by using a graphite lid and then the argon was purged into the crucible for 5 min. The SHS initiation was performed by passing electricity through the resistance wire. After completing the reaction, the crucible was left to soak keeping the argon gas flowing for 30 min. The SHS product was discharged, crushed, and ring milled. In the leaching step, the SHS product was reacted with aqueous acid solution which contains 2 times the stoichiometric amount of HCl acid (5.8 M HCl) at 80 °C and 1 hour using 1/10 solid/liquid ratio in order to dissolve unwanted byproducts (i.e. MgO and Mg₃B₂O₆) from the tungsten

* Corresponding author. Tel.: +90-212-2853367; fax: +90-212-2853427.
E-mail address: bderin@itu.edu.tr (B.Derin)

boride compounds. At the end of the experiments, filter cake was obtained by vacuum solid-liquid separation method washing the leached product with water to neutralize the leaching acid. In the second SHS step, the leached product was again reacted with same amount of the B_2O_3 and Mg mixture keeping same molar ratio of B_2O_3 :Mg (3:8). Then, the similar subsequent acid leaching (5.8 M HCl) on the second SHS product was carried out to eliminate the byproducts. The whole process flow of the experiment is shown in Fig. 1.

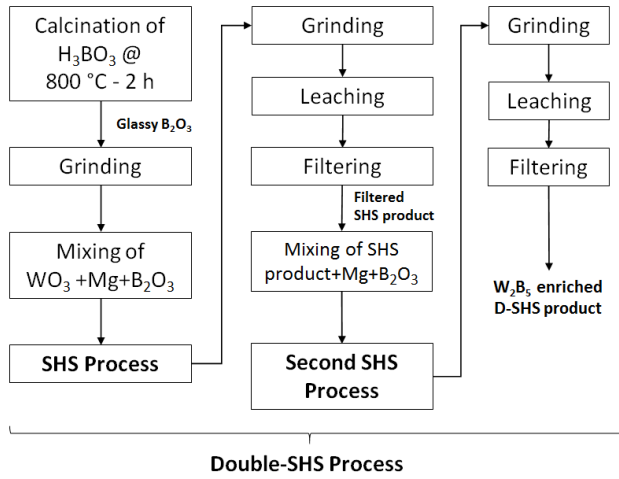


Fig. 1. The process flow of the D-SHS experiment

The phase compositions of the SHS products and filter cakes were examined by using X-ray diffractometer with scanning range of 20° – 80° and scanning rate of $1.54^\circ/\text{min}$ (XRD, PANalytical PW3040/60 with a Cu K α radiation, $\lambda = 1.5406 \text{ \AA}^\circ$) at room temperature. The Rietveld analysis was applied to X-ray diffraction data to calculate the phase compositions by using X'Pert HighScore Plus software. The microstructure of the D-SHS product was characterized by MultiBeam Focused Ion Beam-Scanning Electron Microscope (FIB-SEM, JEOL JIB-4501). The mean diameters and specific surface areas of the leached SHS products were measured by using particle size analyzer (Malvern Mastersizer 2000).

3. RESULTS AND DISCUSSION

A thermochemical calculation was performed to estimate the T_{ad} value and the possible product composition of the SHS reaction by using the advanced “Equilib” module of FactSage 7.1 [21]. In order to simulate the first SHS reaction, 1 mole of WO_3 and 8 moles of Mg were equilibrated with 3 moles of B_2O_3 . The reactions of the process were assumed as adiabatic ($\Delta H = 0$) and the initial reaction temperature was selected as 25°C . FTlite database was selected in order to detect the intermetallic compounds and solid solutions in the product, whereas all gas, liquid and other stoichiometric solid phases were selected from the FactPS database.

According to the calculations, the T_{ad} value was found as 2147°C and the calculated product composition was estimated to be 64.4 wt.% $Mg_3B_2O_6$, 26.9 wt.% W_2B_5 , and 8.7 wt.% WB in the solid phase and 83.7 wt.% Mg, 7.8 wt.% $(BO)_2$, 5.7 wt.% B_2O_3 , and 1.8 wt% BO in the

gas phase of the system. It was also calculated from the Reaction module of FactSage that even at high T_{ad} value, $Mg_3B_2O_6$ formation occurs due to the strong affinity of free MgO with B_2O_3 (Eq. 1). As a result, high amounts of B_2O_3 in the initial mixture result in not only an increase in B/W ratio in the boride phase but also an increase in $Mg_3B_2O_6$ amount in the SHS product.



XRD scan for the unleached SHS product which are selected for the present study are shown in Fig. 2 [19]. The figure depicts that the phases occurred in SHS product were metallic W, W_2B , WB, W_2B_5 , MgO , and $Mg_3B_2O_6$. However, no WB_4 formation was detected in the product. The Rietveld analysis results given in Table 1 indicate that the quantity of $Mg_3B_2O_6$ was almost two times higher than that of MgO in the SHS product [19]. Fig. 2 b shows that MgO and $Mg_3B_2O_6$ phases were successfully eliminated by subsequent leaching step. The XRD intensities of the obtained phases from highest to lowest were identified to be W_2B_5 , WB, and minor W_2B , and W.

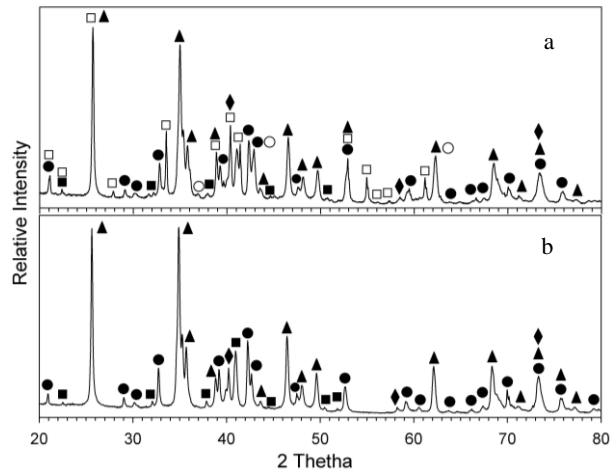


Fig. 2. XRD analysis of a – SHS product [19]; b – leached product [♦W, ■W₂B, ●WB, ▲W₂B₅, ○MgO, □Mg₃B₂O₆] .

According to the Rietveld analysis, after leaching, even though relatively high W_2B_5 /WB weight ratio (~ 4.5) was obtained, almost a quarter of the total amount of the product was composed of the sub-borides, i.e. WB and W_2B , as well as metallic tungsten (Table 1). The mean diameter (d_{50}) and the specific surface area of the leached SHS product were found to be $0.258 \mu\text{m}$ and $21.4 \text{ m}^2/\text{g}$, respectively. In the second stage of SHS experiments, approximately 10 g of the leached product was reacted with the same amount of B_2O_3 and Mg mixture (molar ratio of 3:8). However, the molar ratio for Mg: B_2O_3 in the initial mixture were again selected as 3:8 for keeping the T_{ad} high enough for self-propagation mode. After a successful SHS reaction, the product was then leached in the aqueous acid media. Fig. 3 and Table 1 show the comparison of the XRD patterns and rietveld analysis results of unleached and leached D-SHS products, respectively. The phases occurred in the D-SHS product were WB, W_2B_5 , WB_4 , MgO , and $Mg_3B_2O_6$. No metallic tungsten and W_2B phases were observed in the product.

Table 1. Rietveld analysis of SHS and leached SHS products

Definition	Product composition, wt.-%						
	W	W ₂ B	WB	W ₂ B ₅	WB ₄	MgO	Mg ₃ B ₂ O ₆
SHS product [19]	0.4	1.3	4.8	16.7	—	29.7	61.2
Leached SHS product	2.9	8.4	16.1	72.6	—	—	—
D-SHS product	—	—	0.3	26.7	0.7	43.4	28.9
Leached D-SHS product	—	—	0.6	98.2	1.2	—	—

The quantity of Mg₃B₂O₆ was found lower than that of MgO. It is obvious that lower amount of Mg₃B₂O₆ in the SHS product requires less aggressive leaching conditions, i.e. lower temperature and higher pH values and less time.

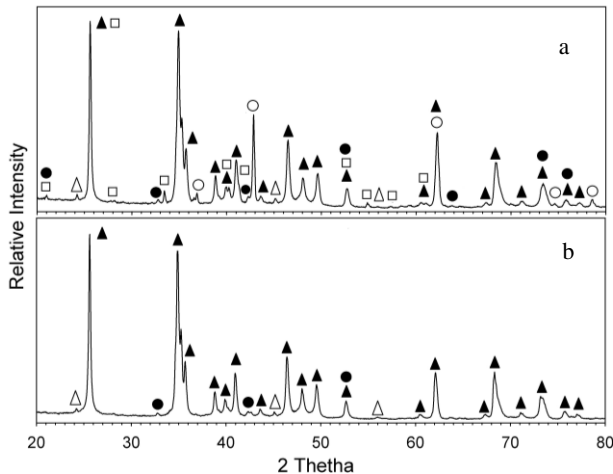


Fig. 3. XRD analysis of a–D-SHS product; b– leached D-SHS product [●WB, ▲W₂B₅, △WB₄, ○MgO, □Mg₃B₂O₆]

The XRD pattern of the leached D-SHS product is shown in Fig. 3 b. After a successful leaching step, no Mg related oxides were detected in the sample. The leached product is mainly composed of W₂B₅ (with major peaks at 2θ = 35.275°, 25.683° and 34.680°, Ref. code 00-038-1365) as well as little amounts of WB₄ and WB, which differs from the first leached one. The Rietveld analysis revealed that approximately 98 wt.% of the resultant product was successfully converted to W₂B₅.

The SEM micrographs at different magnifications of the leached D-SHS product are shown in Fig. 4. The

micrographs confirm that after leaching of MgO and Mg₃B₂O₆ phases, the remaining boride product are porous and composed of nano-sized agglomerated particles which result in higher surface areas. The mean diameter (d₅₀) and the specific surface area of the leached D-SHS product as 0.255 μm and 19.5 m²/g, respectively. These values are very close to those of the leached first SHS product.

The literature indicates that the D-SHS method was used, for the first time, to increase the yield of ZrB₂, since the single SHS of ZrO₂, H₃BO₃ and Mg mixture resulted in an incomplete conversion of ZrO₂ [22]. It was found that, by using D-SHS method, the unreacted ZrO₂ amount decreases only from 37.8 to 16.8 wt.%. However, with the help of the addition of NaCl, the particle size of SHS-ZrB₂ powder (75–125 nm in range) decreases to 25–40 nm after D-SHS. In our study, no diluent such as NaCl and KCl was added to the initial mixtures to modify the particle size.

We must emphasize here that if a boride phase from specific systems such as W-B, Mo-B, and V-B, is aimed to produce via SHS method starting from their oxides, it is mostly probable that the resultant product will contain many stable boride compounds. However, it is possible to increase the ratio of boron to metal in the product by carrying out a second SHS by adding boron oxide and Mg into the system. In the present study, we successfully increased the atomic ratio of boron to tungsten from 1.41 to 2.49 in the boride product after the second SHS process.

Further studies can be conducted to obtain non-agglomerated nano-sized tungsten boride powders with the addition of NaCl as an initial SHS diluents. The effect of B₂O₃/Mg ratio on the D-SHS product should be also considered to obtain high grade of WB₄ compound.

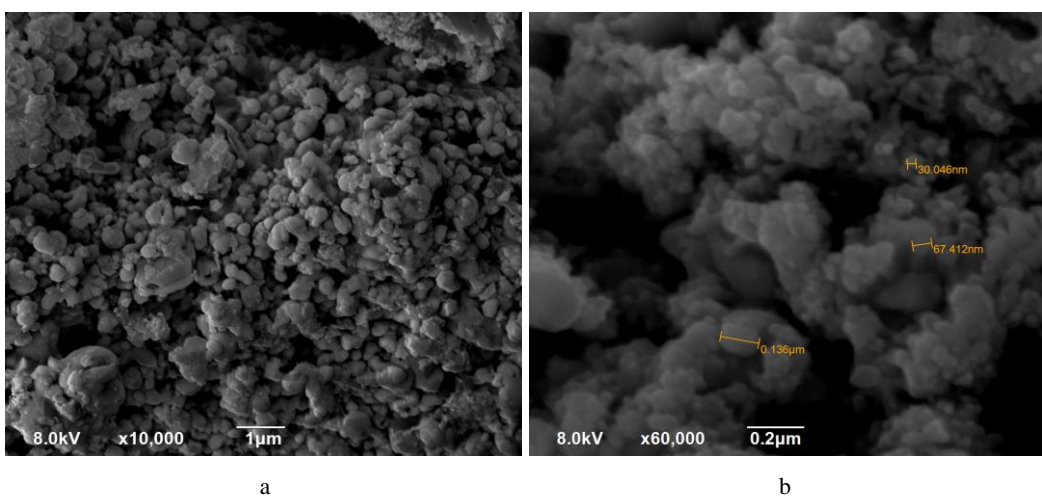


Fig. 4. SEM micrographs of D-SHS product: a–x10000 magnification; b–x60000 magnification

4. CONCLUSIONS

In summary, since the single SHS process from the mixture of $\text{WO}_3\text{:B}_2\text{O}_3\text{:Mg}$ leads to an incomplete conversion to W_2B_5 , some attempts have been made by using Double-SHS method. After the first SHS process of WO_3 and B_2O_3 with magnesiothermic reduction under argon, the tungsten boride compounds were separated from Mg containing by-products by HCl acid leaching. The leached first products were comprised of W, WB, W_2B_5 , and W_2B mixture phases. After the second stage of SHS processing followed by acid leaching, the chemical composition of the leached D-SHS product was found to be 98.2 wt.% W_2B_5 , 1.2 wt.% WB₄, and 0.6 wt.% WB. The specific surface area values of the leached SHS and D-SHS products were found close to each other ($21.4 \text{ m}^2/\text{g}$ and $19.5 \text{ m}^2/\text{g}$, respectively). D-SHS method may be an applicable method to increase boron content in the tungsten boride product.

Acknowledgements

The authors are pleased to acknowledge the financial support for this research from BOREN (Turkish National Boron Research Institute – Project No: 2007.C0064) and Istanbul Technical University Research Foundation.

REFERENCES

1. Zhao, E., Meng, J., Ma, Y., Wu, Z. Phase Stability and Mechanical Properties of Tungsten Borides from first Principles Calculations *Physical Chemistry Chemical Physics* 12 (40) 2010: pp. 13158–13165.
<https://doi.org/10.1039/c004122j>
2. Khor, K.A., Yu, L.G., Sundararajan, G. Formation of Hard Tungsten Boride Layer by Spark Plasma Sintering Boriding *Thin Solid Films* 478 2005: pp. 232–237.
<https://doi.org/10.1016/j.tsf.2004.07.004>
3. Nasiri-Tabrizi, B., Ebrahimi-Kahrizsangi, R., Bahrami-Karkevandi, M. Effect of Excess Boron Oxide on the Formation of Tungsten Boride Nanocomposites by Mechanically Induced Self-Sustaining Reaction *Ceramics International* 40 (9) 2014: pp. 14235–14246.
<https://doi.org/10.1016/j.ceramint.2014.06.013>
4. Bahrami-Karkevandi, M., Ebrahimi-Kahrizsangi, R., Nasiri-Tabrizi, B. Formation and Stability of Tungsten Boride Nanocomposites in $\text{WO}_3\text{-B}_2\text{O}_3\text{-Mg}$ Ternary System: Mechanochemical Effects *International Journal of Refractory Metals and Hard Materials* 46 2014: pp. 117–124.
<https://doi.org/10.1016/j.ijrmhm.2014.05.020>
5. Yeh, C.L., Wang, H.J. Preparation of Tungsten Borides by Combustion Synthesis Involving Borothermic Reduction of WO_3 *Ceramics International* 37 (7) 2011: pp. 2597–2601.
<https://doi.org/10.1016/j.ceramint.2011.04.006>
6. Stadler, S., Winarski, R.P., MacLaren, J.M., Ederer, D.L., vanEk, J., Moewes, A., Grush, M.M., Callcott, T.A., Perera, R.C.C. Electronic Structures of the Tungsten Borides WB, W_2B and W_2B_5 *Journal of Electron Spectroscopy and Related Phenomena* 110–111 2000: pp. 75–86.
[https://doi.org/10.1016/S0368-2048\(00\)00158-4](https://doi.org/10.1016/S0368-2048(00)00158-4)
7. Cai, K.F., Nan, C.W. The Influence of W_2B_5 Addition on Microstructure and Thermoelectric Properties of BaC Ceramic *Ceramics International* 26 (5) 2000: pp. 523–527.
[https://doi.org/10.1016/S0272-8842\(99\)00089-9](https://doi.org/10.1016/S0272-8842(99)00089-9)
8. Dash, T., Nayak, B.B. Preparation of Multi-Phase Composite of Tungsten Carbide, Tungsten Boride and Carbon by Arc Plasma Melting: Characterization of Melt-Cast Product *Ceramics International* 42 (1) 2016: pp. 44445–44459.
<https://doi.org/10.1016/j.ceramint.2015.08.129>
9. Lech, A.T., Turner, C.L., Mohammadi, R., Tolbert, S.H., Kaner, R.B. Structure of Superhard Tungsten Tetra boride: A Missing Link Between MB_2 and MB_{12} Higher Borides *Proceedings of the National Academy of Sciences of the United States of America* 112 (11) 2015: pp. 3223–3228.
<https://doi.org/10.1073/pnas.1415018112>
10. Chrzanowska, J., Kurpaska, L., Giżyński, M., Hoffman, J., Szymański, Z., Mościcki, T. Fabrication and Characterization of Superhard Tungsten Boride Layers Deposited by Radio Frequency Magnetron Sputtering *Ceramics International* 42 (10) 2016: pp. 12221–12230.
<https://doi.org/10.1016/j.ceramint.2016.04.166>
11. Ingole, S., Liang, H., Usta, M., Bindal, C., Ucisik, A.H. Multi-Scale Wear of a Boride Coating on Tungsten *Wear* 259 2005: pp. 849–860.
<https://doi.org/10.1016/j.wear.2004.12.024>
12. Lassner, E., Schubert, V.D. Tungsten: Properties, Chemistry, Technology of the Element, Alloys, and Chemical Compounds. Kluwer Academic/Plenum Publishers, New York, 1999: pp. 138–139.
<https://doi.org/10.1007/978-1-4615-4907-9>
13. Mohammadi, R., Lech, A.T., Xie, M., Weaver, B.E., Yeung, M.T., Tolbert, S.H., Kaner, R.B. Tungsten Tetra boride, an Inexpensive Superhard Material *Proceedings of the National Academy of Sciences of the United States of America* 108 (27) 2011 pp. 10958–10962.
<https://doi.org/10.1073/pnas.1102636108>
14. Khina, B.B. Chemistry Research and Applications Series - Combustion Synthesis of Advanced Materials, Nova Science Publishers, Inc. New York, 2010.
15. Camurlu, H.E., Maglia, F. Preparation of Nano-Size Zrb_2 Powder by Self-Propagating High-Temperature Synthesis *Journal of the European Ceramic Society* 29 2009: pp. 1501–1506.
<https://doi.org/10.1016/j.jeurceramsoc.2008.09.006>
16. Khanra, A.K., Pathak, L.C., Mishra, S.K., Gonkhindi, M.M. Effect of NaCl on the Synthesis of TiB_2 Powder by a Self-Propagating-High-Temperature Synthesis (SHS) Technique *Materials Letters* 58 (5) 2004: pp. 733–738.
<https://doi.org/10.1016/j.matlet.2003.06.003>
17. Nersisyan, H.H., Lee, J.H., Won, C.W. A study of Tungsten Nanopowder Formation by Self-Propagating High-Temperature Synthesis *Combustion and Flame* 142 2005: pp. 241–248.
<https://doi.org/10.1016/j.combustflame.2005.03.012>
18. Yazici, S., Derin, B. Production of Tungsten Boride from CaWO_4 by Self-propagating High-Temperature Synthesis followed by HCl Leaching *International Journal of Refractory Metals and Hard Materials* 29 2011: pp. 90–95.
<https://doi.org/10.1016/j.ijrmhm.2010.08.005>
19. Yazici, S., Derin, B. Effects of Process Parameters on Tungsten Boride Production from WO_3 by Self-Propagating High Temperature Synthesis *Materials Science and Engineering: B* 178 (1) 2013: pp. 89–93.
<https://doi.org/10.1016/j.mseb.2012.10.008>
20. Lv, Y., Wen, G., Lei, T.Q. Friction and Wear Behavior of C-Based Composites in Situ Reinforced with W_2B_5 *Journal of the European Ceramic Society* 26 (15) 2006: pp. 3477–3486.
<https://doi.org/10.1016/j.jeurceramsoc.2005.09.031>
21. Bale, C.W., Bélisle, E., Chartrand, P., Deckerov, S.A., Eriksson, G., Gheribi, A.E., Hack, K., Jung, I.H., Kang, Y.B., Melançon, J., Pelton, A.D., Petersen, S., Robelin, C., Sangster, J., Spencer, P., Van Ende, M.A. FactSage Thermochemical Software and Databases 2010–2016 *Calphad* 54 2016: pp. 35–53.
22. Khanra, A.K., Pathak, L.C., Godkhindi, M.M. Double SHS of ZrB_2 Powder *Journal of Materials Processing Technology* 202 2008: pp. 386–390.
<https://doi.org/10.1016/j.jmatprotec.2007.09.007>